Effect of selective laser sintering on stress relaxation in PA12*)
(Rapid communication)

Wiktor Szot[1), **)] (ORCID ID: 0000-0001-9512-9680), **Jerzy Bochnia**[1)] (0000-0001-7540-3822), **Paweł Zmarzły**[1)] (0000-0003-3717-1500)

DOI: https://doi.org/10.14314/polimery.2024.3.5

Abstract: Effect of selective laser sintering printing orientation (0°, 45°, 90°) on stress relaxation in PA12 was investigated. The results were highly consistent with the Maxwell-Wiechert model, as evidenced by the average values of the fit coefficients $\overline{Chi}^2$ = 0.00004 and $\overline{R}^2$ = 0.996. By changing the printing orientation, anisotropy of rheological properties was achieved.

Keywords: SLS, Maxwell-Wiechert model, stress relaxation, PA12.

Wpływ selektywnego spiekania laserowego na relaksację naprężeń w PA12
(Komunikat szybkiego druku)

Streszczenie: Zbadano wpływ orientacji wydruku selektywnego spiekania laserowego (0°, 45°, 90°) na relaksację naprężeń w PA12. Uzyskano dużą zgodność wyników z modelem Maxwella-Wiecherta, o czym świadczą średnie wartości współczynników dopasowania $\overline{Chi}^2$ = 0,00004 oraz $\overline{R}^2$ = 0,996. Zmieniając orientację wydruku uzyskano anizotropię właściwości reologicznych.

Słowa kluczowe: SLS, model Maxwella-Wiecherta, relaksacja naprężeń, PA12.

The additive technologies found increased usage in various fields of industry, especially where demand for complex shaped parts is growing. For this reason, it is required to conduct extensive research focused on the properties of materials used for 3D printing especially for polymeric materials [1, 2]. Most polymeric materials are chosen more frequently because of their good mechanical properties relative to the low cost of manufacture [3]. Components made of polymers and polymer composites meet the strength requirements while reducing their weight, which is important in the automotive and space industries. The widespread use of polymers for components that operate under constant loads determines the knowledge of the strain-stress relationship. These relationships are needed to conduct stability analyses of details operating under constant stress. Therefore, to determine the reliability and durability of polymer material, it is necessary to know its mechanical properties during its use [3, 4].

Stress relaxation of additively manufactured polymer materials are increasingly being researched [3, 5–12]. To describe the stress relaxation, well-known rheological models are used [5, 13–18]. In authors previous work, research on the rheological properties of parts produced by FDM technology from acrylonitrile-butadiene-styrene (ABS) material was conducted [10]. The samples were subjected to tensile stress and the 3D printing technological parameters analyzed were layer height (0.254 mm and 0.33 mm) and print orientation (0°, 45°, 90°). The Maxwell-Viechert and Kelvin-Voight models were used to describe stress relaxation and material creep, respectively. The results of the research confirmed the obtaining of a strong fit of the rheological models to the experimental curves. Anisotropy of the rheological properties was detected due to the orientation of the print. In another paper, Reis *et al*. [8] analyzed stress relaxation and creep phenomena caused by compressive, tensile, and bending stresses. The research was made of G6-Impact nanocomposite material in FFF technology with technological parameters of layer height (0.25 mm), infill (100%) and deposition angle direction (0°/45°/-45°/90°/90°/-45°/45°/0°). The research results showed that the lowest relaxation values

[1)] Kielce University of Technology, Faculty of Mechatronics and Mechanical Engineering, Tysiaclecia Panstwa Polskiego 7, 25-314 Kielce, Poland.

*) The material was presented at the VI Scientific Conference on "Szybkie Prototypowanie, Druk 3D&4D w zastosowaniach inżynierskich", September 14–15, 2023, Warsaw, Poland.

**) Author for correspondence: wszot@tu.kielce.pl

were obtained for bending stress, while the highest values were obtained for tensile stress. For creep, the highest displacement was obtained for tensile stress. On the other hand, the displacement values for bending and compressive stress were similar. Bochnia *et al*. [19] manufactured samples for rheological research using selective laser sintering (SLS) technology from ALUMIDE material, with print parameters: layer height (0.12 mm), energy density (0.056 J/mm^2) and print direction (X, Y, Z). The samples were exposed to tensile stresses, from which stress relaxation and material creep curves were obtained. Five-parameter Maxwell Wiechert and Kelvin-Voight models were used to describe these curves. It was observed that for both stress relaxation and creep, the direction of printing affected the dynamic viscosity coefficients (obtained by fitting rheological models to experimental curves). The strong fits obtained confirmed the usefulness of the Maxwell-Wiechert and Kelvin-Voight models.

In summary, there is a growing interest in rheological research of additively manufactured materials. In a way, this is a necessity resulting from the increasing use of 3D printing for the manufacture of usable components and components important for the overall device, *e.g.*, mechanical seals.

In additive technologies, technological parameters affect the mechanical properties of manufactured parts [20, 21]. And quite often, the influence of print orientation is analyzed, as confirmed by research described in articles [20–25]. Selective laser sintering (SLS) technology uses a laser beam to selectively irradiate and solidify the material in powder form layer by layer until a finished 3D part is obtained [26, 27]. Before irradiating the powder with a laser beam, it must be heated to a high working temperature. The working temperature must not be higher than the melting point of the polymer material, otherwise the powder particles will stick together [26, 28, 29]. After the layer is applied, the material is selectively solidified by further laser heating to the sintering temperature. The next step is to lower the working platform by a preset layer height and the processes again follow in the order: application of powder, solidification of the applied powder. A three-dimensional object is obtained after an appropriate number of powder layers are applied and sintered [26, 28, 29]. Selective laser sintering technology finds its applications in medicine, aerospace, electronics, packaging, military, and automotive industries [26,29].

Polyamides are the most used polymers in selective powder sintering technology [29]. There are three types of such materials polyamide 6 (PA6), polyamide 11 (PA11) and polyamide 12 (PA12) [29]. Crystalline polyamide 12 is easier to sinter with a laser compared to other polymers [26, 29]. Polyamide behaves as a flexible material when the printed part is thin, while when the model is thick then the polymer behaves as a rigid one. The PA12 material exhibits excellent strength, thermal and chemical resistance properties [29].

T a b l e 1. Selected properties of PA12 (PA2200) [30]

Property	Standard	Direction	Value
Young's modulus MPa	ISO 527	X, Y, Z	1650
Tensile strength MPa	ISO 527	X Y Z	48 48 42
Elongation at break %	ISO 527	X Y Z	18 18 4
Flexural modulus MPa	ISO 178	X	1500
Charpy impact strength, kJ/m^2	ISO 179/1eU	X	53
Hardness, D	ISO 7619-1		75
Biocompatibility – EN ISO 10993-1 and USP/level VI/121. Certified for food contact with Directive 2002/72/EC (except alcohol products).			

The aim of the current research is to investigate effect of selective laser sintering printing orientation (0°, 45°, 90°) on stress relaxation in PA12. Additionally, the five-parameter Maxwell-Wiechert model was used for the mathematical description, determination of elastic moduli and dynamic viscosity coefficients.

EXPERIMENTAL PART

Materials

Polyamide 12 (PA12) trade name PA2200, obtained from EOS GmbH Electro Optical Systems (Krailling, Germany) was used (Table 1).

Samples preparation

Samples for stress relaxation testing were developed in CAD (Computer Aided Design) software (sample 1BA according to ISO 527), and saved in a digital file with STL (Surface Tessellation Language) extension using triangulation parameters: deflection (0.0069 mm), angle (5°). The paddles were obtained by SLS technology using EOS Formiga P100 printer (EOS GmbH Electro Optical Systems, Krailling, Germany). The 3D printing parameters are layer thickness (0.1 mm), energy density (0.056 J/mm^2) and print orientation (0°, 45°, 90°). The samples were marked as follows: e.g., SLS – 90°-1 means that the sample was made using SLS technology, the printing orientation was 90°, and the test number was 1. A scheme of the SLS process is shown in Figure 1 [26, 27].

Methods

Stress relaxation

Stress relaxation was tested on the Inspect mini testing machine (Hegewald&Peschke MPT GmbH, Nossen, Germany) at a head speed of 10 mm/s, a constant strain of

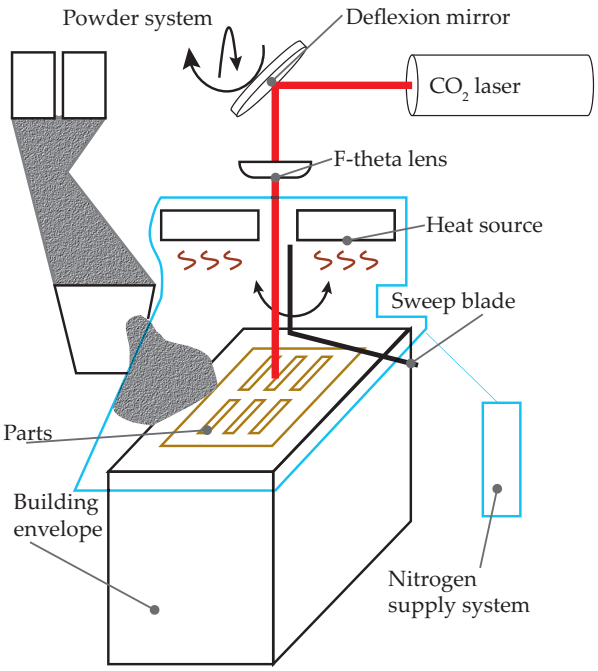

Fig. 1. Scheme of 3D printing process using SLS technology

1 mm and a relaxation time of 600 s. Measurements, data acquisition and test parameter setting were performed in the LabMaster program (version 2.5.3.21).

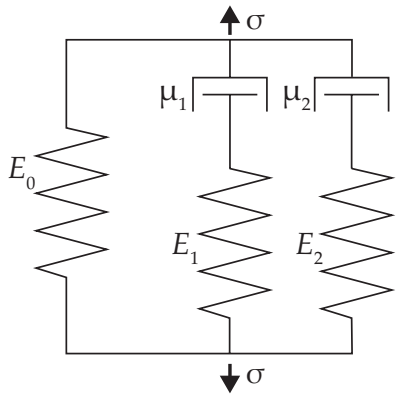

Fig. 2. Schematic diagram of Maxwell-Wiechert model [19]

The Maxwell-Wiechert model

The five-parameter Maxwell-Wiechert model was used to mathematically describe the experimental curves obtained in stress relaxation tests. Fitting was performed using OriginPro software (OriginLab Corp., Northampton, Massachusetts, USA) with the Levenberq-Marquadt algorithm. Schematic diagram of the Maxwell-Wiechert model is shown in Fig. 2 [9, 10, 19].

The Maxwell-Wiechert model can be described using Equation 1 [10, 19]:

T a b l e 2. Parameters and fitting factors for PA12 samples

Sample	σ_0, MPa	σ_1, MPa	σ_2, MPa	t_1, s	t_2, s	Chi^2	R^2
SLS – 0°-1	4.86	0.92	0.90	10.83	221.09	0.00004	0.995
SLS – 0°-2	5.00	0.94	0.91	10.45	210.64	0.00004	0.995
SLS – 0°-3	5.16	0.95	1.00	10.65	206.90	0.00004	0.996
SLS – 0°-4	5.50	0.97	1.01	10.14	210.65	0.00004	0.996
SLS – 0°-5	5.70	0.99	1.10	9.73	218.05	0.00004	0.996
$\bar{x}$	5.24	0.95	0.98	10.36	213.47	0.00004	0.996
SD	0.35	0.03	0.08	0.44	5.88	0.0000	0.001
SLS – 45°-1	5.89	0.84	0.89	11.23	218.87	0.00004	0.995
SLS – 45°-2	5.70	1.00	1.05	14.16	328.30	0.00004	0.992
SLS – 45°-3	6.30	1.04	1.19	12.41	263.44	0.00005	0.997
SLS – 45°-4	5.83	0.97	0.98	11.67	248.63	0.00005	0.994
SLS – 45°-5	5.90	1.04	1.10	11.70	236.99	0.00004	0.995
$\bar{x}$	5.92	0.98	1.04	12.23	259.25	0.00004	0.995
SD	0.22	0.08	0.11	1.16	41.91	0.00001	0.002
SLS – 90°-1	5.09	0.90	0.80	11.11	216.49	0.00004	0.994
SLS – 90°-2	5.99	1.04	1.02	11.58	212.20	0.00004	0.995
SLS – 90°-3	5.52	0.97	0.96	11.51	213.30	0.00004	0.995
SLS – 90°-4	5.58	0.98	0.98	10.85	218.62	0.00004	0.995
SLS – 90°-5	5.77	0.95	0.93	11.26	212.67	0.00004	0.995
$\bar{x}$	5.59	0.97	0.94	11.26	214.66	0.00004	0.995
SD	0.33	0.05	0.08	0.30	2.78	0.00000	0.000

T a b l e 3. Moduli of elasticity and dynamic viscosity for PA12

Raster angle, °	E_0, MPa	E_1, MPa	E_2, MPa	E_z, MPa	μ_1, MPa·s	μ_2, MPa·s
0	262.20	47.70	49.20	359.10	494	10502
45	296.20	48.90	52.10	397.20	598	13507
90	279.50	48.40	46.90	374.80	545	10067

$$\sigma(t) = \varepsilon_0 E_0 + \varepsilon_0 E_1 e^{\frac{-E_1 t}{\mu_1}} + \varepsilon_0 E_2 e^{\frac{-E_2 t}{\mu_2}} \quad (1)$$

where: E_0, E_1, E_2 – moduli of elasticity, μ_1, μ_2 – dynamic viscosity coefficients, ε_0 – initial unit strain, t – time.

Equation 1 can be simplified and then takes the form of Equation 2 [19]:

$$\sigma(t) = \sigma_0 + \sigma_1 e^{\frac{-t}{t_1}} + \sigma_2 e^{\frac{-t}{t_2}} \quad (2)$$

where: $t_1 = \frac{\mu_1}{E_1}$ – relaxation time, $t_2 = \frac{\mu_2}{E_2}$ – relaxation time,

In addition, the equivalent modulus was calculated according to Equation 3 [19]:

$$E_z = E_0 + E_1 + E_2 \quad (3)$$

The percentage decrease in stress after a given exposure time was calculated according to Equation 4:

$$\sigma(t) = \frac{\sigma_0 - \sigma_t}{\sigma_0} \cdot 100\% \quad (4)$$

where: σ_0 – initial stress, σ_t – stress after time t.

RESULTS AND DISCUSSION

Experimental stress relaxation curves at different printing orientation are presented in Figure 3. Selected experimental relaxation curves fitted to the Maxwell-Wiechert model are shown in Figure 4.

The result of the approximation was the model parameters Maxwell-Wiechert σ_0, σ_1, σ_2, t_1, and t_2 and the fitting coefficients Chi^2 and R^2. The values of these parameters and coefficients are presented in Table 2.

Based on the results presented in Table 2, the highest standard deviation was obtained for the parameter t_2 (41.96 s) and printing orientation of 45°. The parameter t_2 obtained the highest standard deviation among the others. The lowest standard deviation was obtained for the parameter σ_1 (0.03 MPa). In the case of matching coefficients, standard deviations reached low values.

Using the average values of the parameters $\overline{\sigma}_0$, $\overline{\sigma}_1$, $\overline{\sigma}_2$, $\overline{t}_1$, and $\overline{t}_2$ and the given constant strain (ε_{const} = 1 mm) the elastic moduli E_0, E_1, E_2 and the dynamic viscosity coefficients μ_1, μ_2 were calculated. The values of elastic moduli and dynamic viscosity coefficients along with the equivalent modulus are presented in Table 3.

The elastic moduli did not differ much depending on the printing orientation. The highest elastic modulus, equivalent modulus and dynamic viscosity coefficients were obtained with a print orientation of 45°. The dynamic viscosity coefficient μ_1 did not vary much depending on print orientation. However, in the case of μ_2, high difference between the highest and the lowest value was observed.

Table 4 shows that the largest standard deviation occurred at a print orientation of 45°, and the lowest at a print orientation of 90°. The overlap of the experimental curves (black) and the rheological model curves (red) confirms a very good fit (Fig. 4), as also evidenced by the values of the fit coefficients R^2 and Chi^2. The closer Chi^2 parameter is to 0, the better the fit. For R^2, the fit is better when its value is closer to 1. The average Chi^2 and R^2 values for the tested samples were 0.0004 and 0.996, respectively. Moreover, it is observed that the highest equivalent modulus (397 MPa) was 10% higher than the lowest E_Z (359 MPa). For the dynamic viscosity coefficient μ_2, the highest value of 13507 MPa·s was 25% higher than the lowest value of 10067 MPa·s. For the dynamic viscosity coefficient μ_1, the highest value of 598 MPa·s was 17% higher than the lowest value of 494 MPa·s. Analyzing the relaxation time t_2, the highest standard deviation (41.9 s) was achieved for a printing orientation of 45° and it was 93% higher than the lowest (2.8 s) obtained for a printing orientation of 90°.The high SD of the time t_2 is caused by the different dynamic viscosity coefficient μ_2.

The elastic moduli and dynamic viscosity coefficients were related to the research presented elsewhere [31]. The authors applied compressive stress to cylindrical specimens. They obtained elastic moduli and dynamic viscosity coefficients for printing orientation of 0° and 90°. The samples were made from PA12 using SLS technology. The comparison shows that the elastic modulus E_0 was 2.7 times higher for tensile stress compared to compressive stress. In contrast, the elastic moduli E_1, E_2 were on average 16.5 times higher for tensile stress compared to compressive stress. The reverse was true

Table 4. Stress drops after exposure time of PA12 samples

Test number	Decrease in stress, %		
	0°	45°	90°
1	33.5	29.2	31.3
2	33.1	31.7	31.2
3	33.3	30.9	31.7
4	32.0	30.5	31.6
5	31.8	32.3	30.4
$\overline{x}$	32.7	30.9	31.3
SD	0.8	1.2	0.5

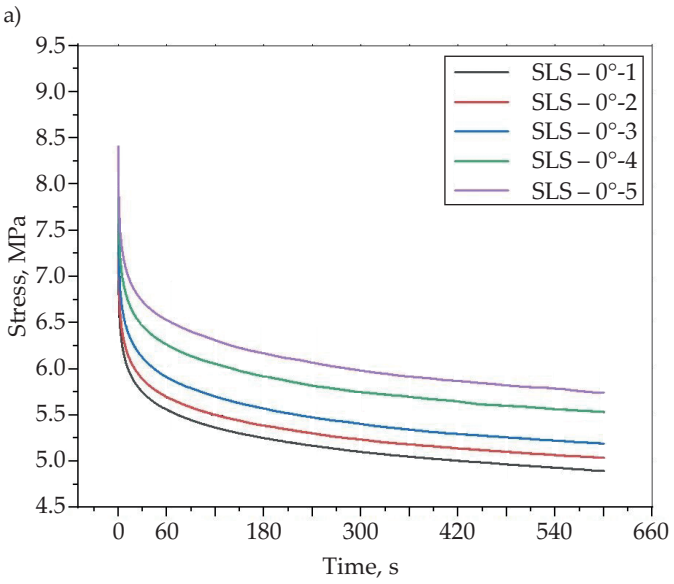

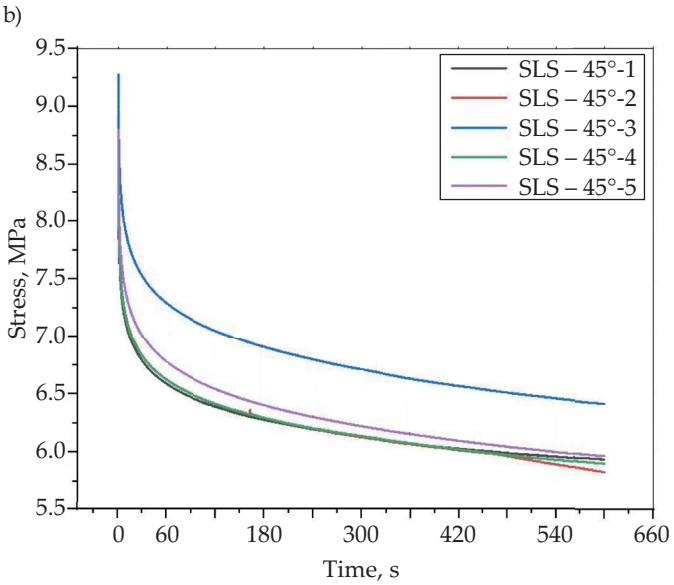

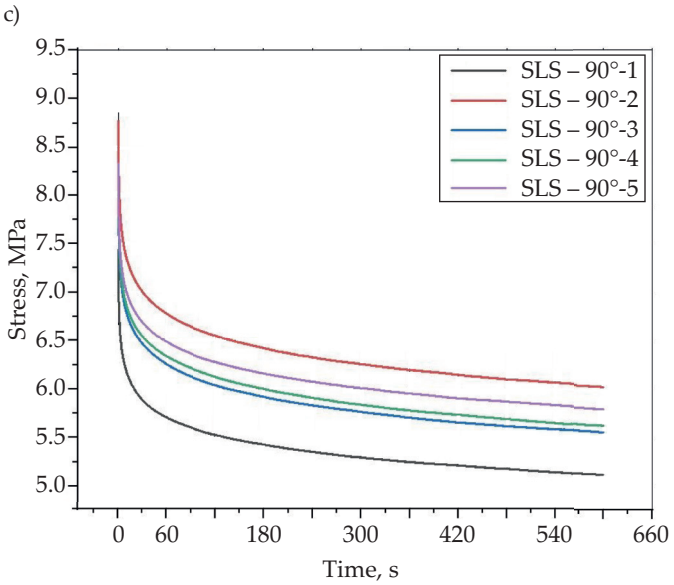

Fig. 3. Experimental stress relaxation curves at different printing orientation: a) 0°, b) 45°, c) 90°

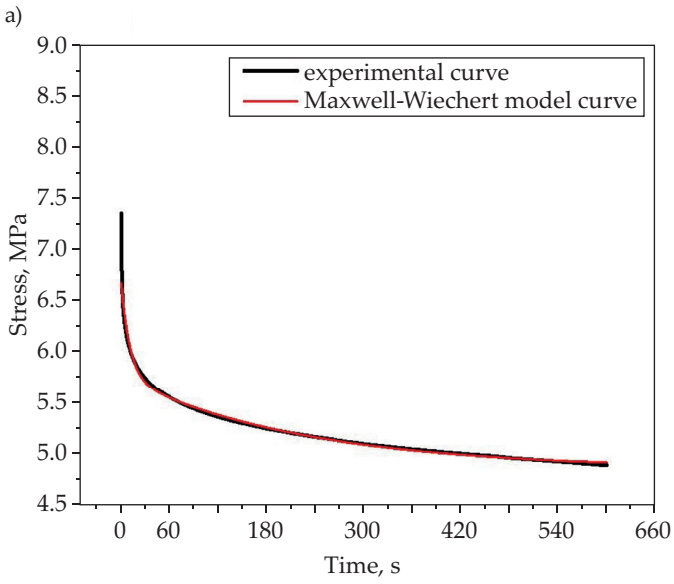

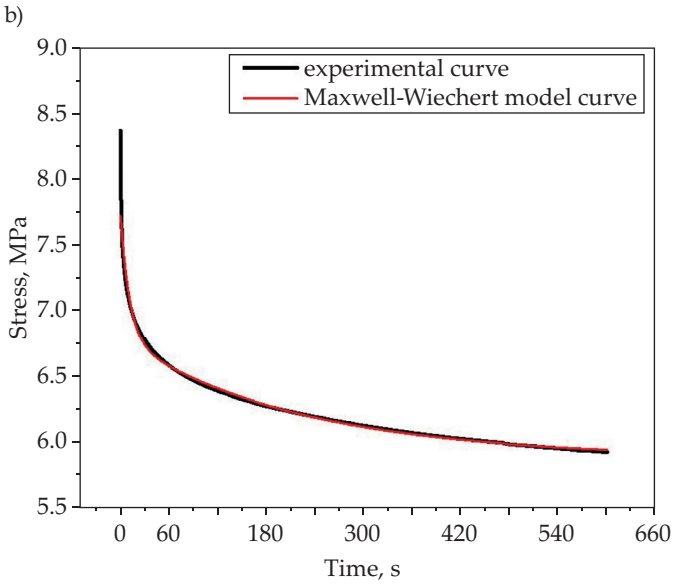

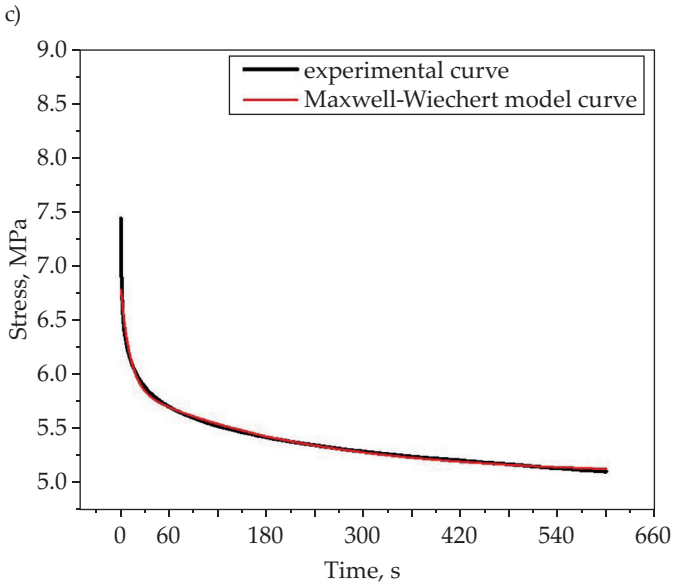

Fig. 4. Selected experimental data fitted to the Maxwell-Wiechert model: a) SLS – 0°-1, b) SLS – 45°-1, c) SLS – 90°-1

for dynamic viscosity coefficients μ_1, μ_2, which were on average 1.5 times higher for compressive stress compared to tensile stress.

CONCLUSIONS

The influence of SLS printing orientation on stress relaxation in PA12 was investigated. The obtained results fit the Maxwell-Wiechert model very well, as evidenced by the average values of the coefficients, which were $\overline{Chi}^2$ (0.0004) and $\overline{R}^2$ (0.996). This allows to recommend the obtained results for various engineering calculations, especially computer simulations with practical utilitarian applications. It was found that the anisotropy of rheological properties results from the printing orientation. The decrease in relaxation stress was the highest for a print orientation of 0° (32.7%), which suggests that this printing orientation is the least favorable for structural elements that maintain, for example, tightness or fastening.

Author contribution

W.S. – conceptualization, data curation, formal analysis, investigation, resources, validation, visualization, writing; J.B. – conceptualization, validation; P.Z – conceptualization, validation.

Funding

The financial support from the government, industry or any other source, has been acknowledged in the paper. No funding.

Conflict of interest

The authors declare no conflict of interest.

REFERENCES

[1] Oleksy M., Budzik G., Sanocka-Zajdel. *et al*.: *Polimery* **2018**, *63(7-8)*, 531. https://doi.org/10.14314/polimery.2018.7.7
[2] Kroczek K., Turek P., Mazur D. *et al*.: *Polymers* **2022**, *14(8)*, 1526. https://doi.org/10.3390/polym14081526
[3] Ibrulj J., Dzaferovic E., Obucina M.: "Determination of Relaxation and Creep Modulus of Polymer Materials Obtained by 3D Printing" in "New Technologies, Development and Application III", Springer, Cham 2020. p. 256. https://doi.org/10.1007/978-3-030-46817-0_29
[4] Ibrulj J., Dzaferovic E., Obucina M. *et al*.: *Polymers* **2021**, *13(19)*, 3276. https://doi.org/10.3390/polym13193276
[5] Lin C.-Y., Chen Y.-C., Lin C.-H. *et al*.: *Polymers* **2022**, *14(10)*, 2124. https://doi.org/10.3390/polym14102124
[6] Zheng J.H., Jin Y., Xu L. *et al*.: *Metals* **2023**, *13(4)*, 778. https://doi.org/10.3390/met13040778
[7] Tüfekci K., Çakan B.G., Küçükakarsu, V.M.: *Journal of Applied Polymer Science* **2023**, 140(39), e54463. https://doi.org/10.1002/app.54463
[8] Reis P.N.B., Valvez S., Ferreira J.A.M.: *Procedia Structural Integrity* **2022**, *37*, 934. https://doi.org/10.1016/j.prostr.2022.02.028
[9] Bochnia J., Kozior T., Szot W. *et al*.: *3D Printing and Additive Manufacturing* **2022**. https://doi.org/10.1089/3dp.2022.0215
[10] Szot W.: *3D Printing and Additive Manufacturing* **2023.** https://doi.org/10.1089/3dp.2022.0298.
[11] Hu R., Zhang X., Chen Y. *et al*.: *Additive Manufacturing* **2022**, *50*, 102583. https://doi.org/10.1016/j.addma.2021.102583
[12] Pascual-Francisco J.B., Susarrey-Huerta O., Farfan-Cabrera L.I. *et al*.: *Fractal and Fractional* **2023**, *7(8)*, 568. https://doi.org/10.3390/fractalfract7080568
[13] Pacheco J.E.L., Bavastri C.A., Pereira J.T.: *Latin American Journal of Solids and Structures* **2015**, *12*, 420. https://doi.org/10.1590/1679-78251412
[14] Jayswal A., Liu J., Harris G. *et al*.: *Polymer Engineering and Science* **2023**, *63(11)*, 3809. https://doi.org/10.1002/pen.26486
[15] Valvez S., Silva A.P., Reis P.N.B.: *Aerospace* **2022**, *9(3)*, 124. https://doi.org/10.3390/aerospace9030124
[16] Bochnia J., Blasiak S.: *MM Science Journal* **2020**, *March*, 3774. https://doi.org/10.17973/mmsj.2020_03_2019122
[17] Kozior T., Kundera C.: *Polymers* **2021**, *13(11)*, 1895. https://doi.org/10.3390/polym13111895
[18] Bochnia J.: *Procedia Engineering* **2012**, *39*, 98. https://doi.org/10.1016/j.proeng.2012.07.013
[19] Bochnia J., Blasiak S.: *Polymers* **2020**, *12(4)*, 830. https://doi.org/10.3390/polym12040830
[20] Faidallah R.F., Hanon M.M., Szakál, Z. *et al*.: *Acta Polytechnica Hungarica* **2023**, *20(6)*, 7. https://doi.org/10.12700/aph.20.6.2023.6.1
[21] Ranganathan S., Kumar K.S., Gopal S. *et al*.: *SAE Technical Papers* **2020**. https://doi.org/10.4271/2020-28-0411
[22] Kluczyński J., Śniezek L., Grzelak K. *et al*.: *Bulletin of the Polish Academy of Sciences: Technical Sciences* **2020**, *68(6)*, 1413. https://doi.org/10.24425/bpasts.2020.135396
[23] Boyer R.A., Kasper F.K., English J.D. *et al*.: *American Journal of Orthodontics and Dentofacial Orthopedics* **2021**, *160(5)*, 732. https://doi.org/10.1016/j.ajodo.2021.01.018

[24] Fisher T., Almeida J.H.S., Falzon B.G. *et al.*: *Polymers* **2023**, *15(7)*, 1708. https://doi.org/10.3390/polym15071708
[25] Ngoc N.V., Khai N.K., Tung N.V. *et al.*: "A Review of the Mechanical of SLA 3D Printing Materials: Printing Orientations and Photopolymerization Technology" in "AMAS 2021: Proceedings of the International Conference on Advanced Mechanical Engineering, Automation, and Sustainable Development 2021", Springer, Cham 2022. p. 660. https://doi.org/10.1007/978-3-030-99666-6_95
[26] El Magri A., Bencaid S.E., Vanaei H.R. *et al.*: *Polymers* **2022**, *14(17)*, 3674. https://doi.org/10.3390/polym14173674
[27] Marsavina L., Stoia D.I.: *Material Design and Processing Communications* **2020**, *2(1)*, 1. https://doi.org/10.1002/mdp2.112
[28] Guo X., Moudgil B.M.: *KONA Powder and Particle Journal* **2023**, *12*, 2024012. https://doi.org/10.14356/kona.2024012.
[29] Han W., Kong L., Xu M.: *International Journal of Extreme Manufacturing* **2022**, *4*, 042002. https://doi.org/10.1088/2631-7990/ac9096.
[30] https://www.eos.info/en/3d-printing-materials/plastic/polyamide-pa-12-alumide (access date 15.11.2023)
[31] Bochnia J., Blasiak S.: *Rapid Prototyping Journal* **2019**, *25*, 76. https://doi.org/10.1108/rpj-11-2017-0236

Received 14 XI 2023.
Accepted 13 XII 2023.